Embedded antennas for signal-transmissive-walls in radio-connected low-energy urban buildings

Alejandra Garrido Atienza

Advisor: Katsuyuki Haneda
Supervisor: Juan Manuel Rius

Master's Thesis submitted to the School of the ETSETB
in partial fulfillment of the requirements for the degree of

Master in Telecommunication Engineering

Universitat Politècnica de Catalunya
January 2020

Table of contents

List of figures

List of tables

List of Acronyms

L attenuation

σ conductivity

EM electromagnetic

mmW millimeter-wave

ε_r^* relative permittivity

ε_r' relative permittivity real part

TIR total internal reflection

Acknowledgement

This thesis would not be possible without the contribution and help in different ways from many people. First of all, I would like to thank Professors Katsuyuki Haneda and Clemens Icheln for giving me the opportunity during my exchange at Aalto University to stay in their group during my master thesis. Also, my group colleges, Mikko and Lauri, for helping me during my work, I've learnt a lot from them. I also would like to thank my partner, Christian to help me to improve my confidence when I was too stressed. Finally, but not less important, of course to my family, special mention to my mum who always believes in me.

Abstract

The work presented in this thesis intends to develop an accurate method to study how to improve the cellular indoor coverage in Finnish buildings. The goal of this method is to have an accurate way to simulate any kind of building wall in order to be able to design different systems to improve the cellular indoor coverage. First of all the characterization of the electromagnetic properties (permittivity and conductivity) of typical building materials are presented. Following with a reference wall study in both, analytical and 3D full-wave method. Finally to prove that the method is consistent and it works, two solutions are developed to improve the 5G signal indoor coverage in the Finnish buildings. Two frequency ranges of the 5G spectrum are considered relevant, sub-6 GHz and millimeter-wave (mmW).

The first proposed solution is a planar antenna, well-known for its low profile, which suits perfectly embedded into the walls. The second proposal is a dielectric wave-guide, interesting approach due to the non-metallic materials. The absence of metallic materials could be beneficial as it preserves the thermal isolation properties of the outer wall.

Chapter 1

Introduction

1.1. Motivation

Ensuring cellular radio coverage is a prerequisite in realizing wireless services and applications. Among different environment where there is a quality of services requisites, in-building sites have become one of the challenging environments, as concrete, almost always present in walls of the buildings, has high radio wave attenuation. Nowadays is becoming more important as Finnish building industry is moving towards the zero-energy buildings to save energy consumption to heat the buildings, this could include different materials in the walls, including some metal or aluminum foil.

Another aspect to take into account is that society is moving towards 5G and at those frequencies the attenuation is much more important. The demanding applications of future 5G networks entail the necessity of finding innovative solutions clearly above from the crowded spectrum below 6 GHz, enabling bandwidths up to a few GHz. This has motivated engineers to move up in frequency and, millimeter-wave bands are the next frontier for both, regulators and cellular industry.

The use of millimeter-wave bands represents a challenge from many points of view, but it is an almost unexplored region of the spectrum for mobile communications, which could benefit. The most important strength is the available bandwidth. It needs to be regulated first to allocate all requesting candidates but, once the spectrum is divided, an enormous potential can be exploited to establish ultra-fast and massive links. Another advantage is that 5G is still far from very energetic frequencies, so it is harmless and suitable for other applications such as tomography [2, 3] and radar imaging [4, 5].

On the other hand, the most limiting factor for using millimeter-wave is the high atmospheric attenuation and the even larger transmission losses in the outer walls of buildings, where cellular users are nowadays expecting as good coverage as outside. Therefore it is important to study different options to improve the cellular coverage inside buildings without sacrificing the mechanical strength of the wall nor its thermal insulating properties.

1.2. Objectives

The main goal of this thesis is to define an accurate method to be able to design a system which improves the indoor cellular coverage at typical 5G frequency bands, both at microwave and millimeter-wave frequencies.

The thesis is structured according to the following main contributions:

- Develop efficient and accurate method for simulating the antennas and circuits embedded into building walls from the electromagnetic point of view, and for analyzing their impact on the attenuation of the 5G signals at two relevant frequency bands.
- Design, develop and simulate the two solutions proposed, the microstrip patch antenna system and the dielectric waveguide. Quantify the advantages and drawbacks of each design.
- A conclusive comparison of the two proposed antenna systems.

1.2.1. Work Plan

The project is divided in three main parts:

- The definition and characterization of electromagnetic properties of a reference wall.
- Define, develop and analyze two antenna-system at sub-6 GHz.
- Analyze the two proposed solutions at millimeter-wave frequency band.

In addition, documentation and writing tasks must be carried out as well as the preparation of the final presentation. The following simplified Gantt diagram summarizes in the time domain the main working areas.

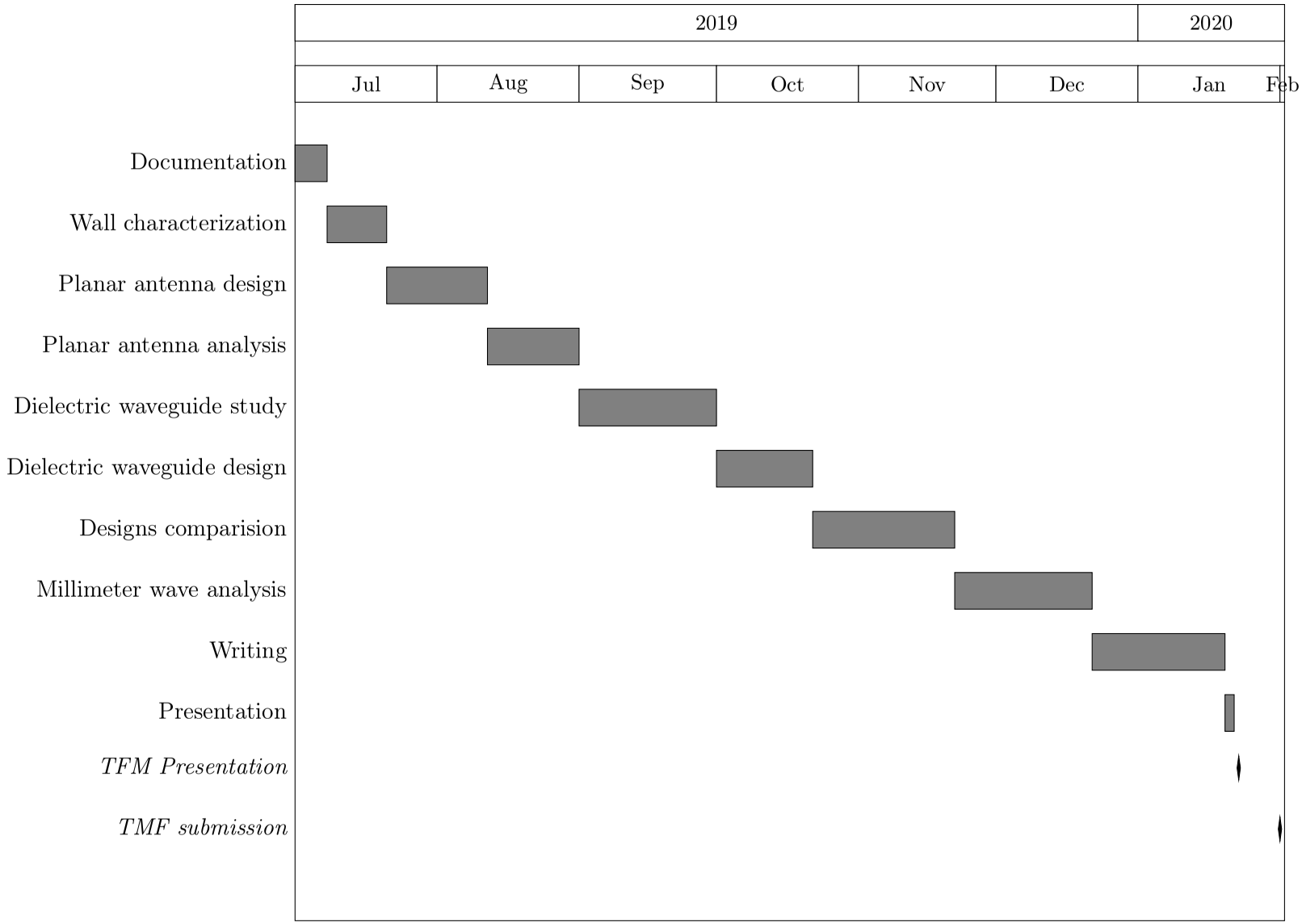
2019
2020
Jul
Aug
Sep
Oct
Nov
Dec
Jan
Feb
Documentation
Wall characterization
Planar antenna design
Planar antenna analysis
Dielectric waveguide study
Dielectric waveguide design
Designs comparision
Millimeter wave analysis
Writing
Presentation
TFM Presentation
TMF submission

Chapter 2

Background and Theory

Typical building walls are composed of several dielectric materials, such as concrete or rock wool. Each one of these materials has different electric and thermal properties. To get more insights about how these materials affect the cellular coverage indoors, the electrical properties of the materials used in walls are explained in section 2.1. Although the thermal analysis is out of the scope of this thesis, the thermal properties of the materials are also taken into account in the antenna design, as the wall must maintain its insulating properties. Thermal insulation aspects of the antenna design are explained in section 2.2. Basic definitions of the figures of merit used in this work are presented in the last section 2.3

2.1. Electrical properties of dielectric materials

When an electromagnetic field propagates in a medium, the field excites a movement of the electric charges composing the medium. Depending on how the charges move, materials can be classified into two types: conductors and dielectrics. In conductor materials, the charges are free of movement. Although in case of dielectric materials, there is a slight shift between positive and negative charges, forming electric dipoles aligned according to the illuminating field, this interaction between forces results in energy storage what is known as polarization.

On the other hand, a dielectric material can be lossless of lossy. In the lossless case, the field is not attenuated whilst in the lossy dielectric the wave is attenuated as it propagates. In this case is convenient to define the complex relative permittivity as described in equation 2.1.

$$\varepsilon_r* = \varepsilon'_r - j\frac{\sigma}{\omega} \tag{2.1}$$

$$\omega = 2\pi f \tag{2.2}$$

where ε'_r is the dielectric constant, σ the conductivity of the material, and ω is the angular frequency of the electromagnetic (EM) field applied.

The real part of the complex relative permittivity is the dielectric constant, which

defines the ability of the media to store electrical energy in an electric field. While the imaginary part reflects the losses caused by the conductivity. There are different ways to describe the losses of a conducting dielectric, but in this work, the attenuation rate, in terms of how many dB is the electric field attenuated when it propagates one meter, as describe equation 2.3, is used.

$$L = 1636\frac{\sigma}{\sqrt{\varepsilon'_r}} \tag{2.3}$$

2.2. Thermal properties of building and antenna materials

Although the thermal analysis of the proposed antenna systems is out of the scope of this thesis, in this section the thermal conductivity is defined and the thermal conductivity values of the materials that are used in this thesis are presented to get an idea about how well justified the proposed designs are.

The thermal conductivity of a material measures the ability to conduct heat. Heat transfer occurs at a lower rate in materials of low thermal conductivity than in materials of high thermal conductivity. This measure is important because one of the goals of the new zero-energy buildings is to reduce the energy used in the buildings, to heat them. Because of that is important to choose also the antenna system materials accordingly, i.e. use materials with low thermal conductivity. Based on the materials used usually in the construction field, the materials for the solutions proposed in this work have been chosen. The different values for the materials used are in the table 2.1 [6] [7].

Table 2.1: Thermal conductivity of dielectric materials used in building industry and in the proposed antenna-circuit systems

Material	**Thermal conductivity** (κ) $\left(\frac{W}{mK}\right)$
Copper	380 (typical conductor in RF circuits)
Rock Wool	0.06 (insulator in building walls)
Reinforced Concrete	2.3 (in load-bearing wallls)
Fiber Glass	0.06 (used in the waveguide)

2.3. Figures of merit

When an electromagnetic field propagates through a boundary between two different media, part of the field will be reflected and the other part of the field will propagate into the second medium. From this latter, some of it will be lost due to the attenuation of the material.

The reflection for the case studied in this work, i.e. normal incidence on the building

walls, is defined by equation 2.4.

$$R = \frac{\sqrt{\varepsilon_{r1}} - \sqrt{\varepsilon_{r2}}}{\sqrt{\varepsilon_{r1}} + \sqrt{\varepsilon_{r2}}} \tag{2.4}$$

When the difference between the dielectric constant of the materials is larger the portion of the field reflected is also larger. It means there will be less power at transmitted. This can be avoided by adding matching layers or systems that make the transition between the dielectric constants smoother.

The transmission coefficient is calculated for all the different proposed setups and compared with the transmission through the reference building wall without any antenna-system embedded.

$$T = 1 - R - L \tag{2.5}$$

In this thesis transmission and reflection are calculated in two different ways: analytically and by 3D full-wave simulations by CST. For the analytical case, the transmission and the reflection are calculated through equations explained in Chapter 3.

On the other hand, the full-wave simulations calculate the scattering parameters (S-Parameters). The scattering parameters describe the electrical behavior of an electrical network. The scattering term refers to the effect observed when a plane wave is incident or passes across different dielectric medium. The S-Parameters describe how the traveling currents and voltages are affected when they find a discontinuity. The S-Parameters are defined in terms of incident and reflected power waves a_i incident wave defined in Eq. 2.6a, and b_i reflected wave defined in Eq. 2.6b, for $i = 1...N$ with N the number of ports in the electrical network.

$$a_i = \frac{1}{2}\frac{(V_i + Z_0 I_i)}{\sqrt{|\operatorname{Re}(Z_0)|}} \tag{2.6a}$$

$$b_i = \frac{1}{2}\frac{(V_i - Z_0^* I_i)}{\sqrt{|\operatorname{Re}(Z_0)|}} \tag{2.6b}$$

Where the ports have all the same characteristic impedance (Z_0), V_i and I_i are the complex amplitudes of the voltage and current at port i. The relation between the incidence and reflected wave with the scattering parameters is the following:

$$\mathbf{b} = \mathbf{aS} \tag{2.7}$$

Chapter 3

Electromagnetic model of the wall

There are many different kinds of building walls, e.g. depending on the country. If it is a cold country building wall will have to provide more insulation, as in Finland. Another aspect is their function, for example, if it is a load-bearing wall or a simple wall to separate rooms. To be able to simulate and compare different solutions a reference wall is needed. In this thesis a typical load-bearing wall structure is presented as a model of reference.

The wall consists of 220 mm-thick rock wool layer for thermal insulation sandwiched by a 70 mm-thick (outer layer) and a 150 mm-thick (inner layer) reinforced concrete for structural bearing. The lateral cross-section of the model is shown in Figure 3.1.

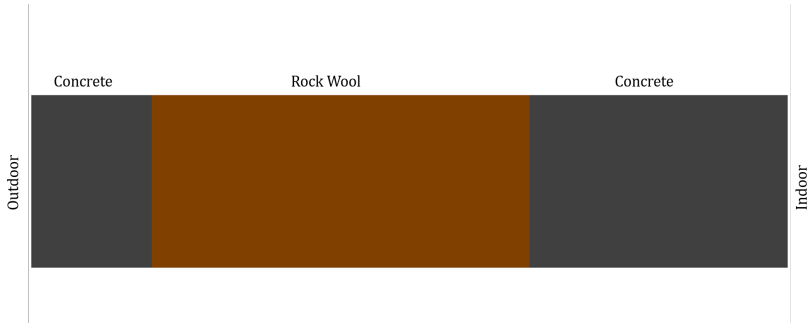

Figure 3.1: Load bearing wall structure (lateral cross-section view)

The reinforced concrete is based on standard concrete with a steel-bar structure inside. There are different types of steel reinforcements depending on the construction company. As a relevant practical case, in this work the steel net mesh size considered is 15 cm x 15 cm with 6 mm thickness [8]. The steel-bar structure is shown at Figure 3.2.

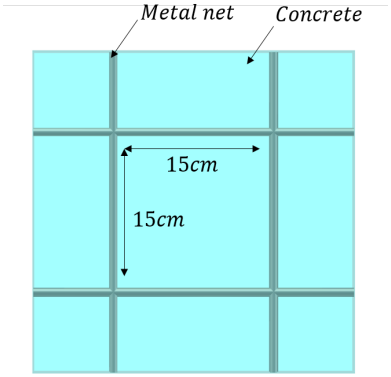

Figure 3.2: Reinforced concrete metal net (front view)

The metal inclusions are not included in the actual transmission evaluation. Nevertheless, to avoid any reflection or interference with the metal-bar, the size of the metal net is used as maximum unit cell size in the simulation settings.

3.1. Electrical properties of building wall materials

The effect of the building materials and structures on radio-wave propagation has been studied in the recommendation from ITU-R P.2040-1 [1]. The recommendation collects electromagnetic measurements of different construction materials, from 1 GHz up to 100 GHz and extrapolates a regression model for each material and its electrical properties in dependence of the frequency: relative permittivity real part (ε'_r) conductivity (σ).

$$\varepsilon'_r = af^b \tag{3.1}$$

$$\sigma = cf^d \tag{3.2}$$

In this project, this regression has been used in order to electromagnetically characterize the concrete and the rock wool. The values of a, b, c and d for concrete and rock wool are listed in Table 3.1.

Table 3.1: Building wall model electrical properties

Material	**Real part of relative permittivity**		**Conductivity (S/m)**		**Frequency Range**
	a	**b**	**c**	**d**	**GHz**
Concrete	5.31	0	0.0326	0.8095	1-100
Rock Wool	1.5	0	0.0005	1.1634	1-100

The dielectric constant and the conductivity of concrete and rock wool are depicted in Figures 3.3

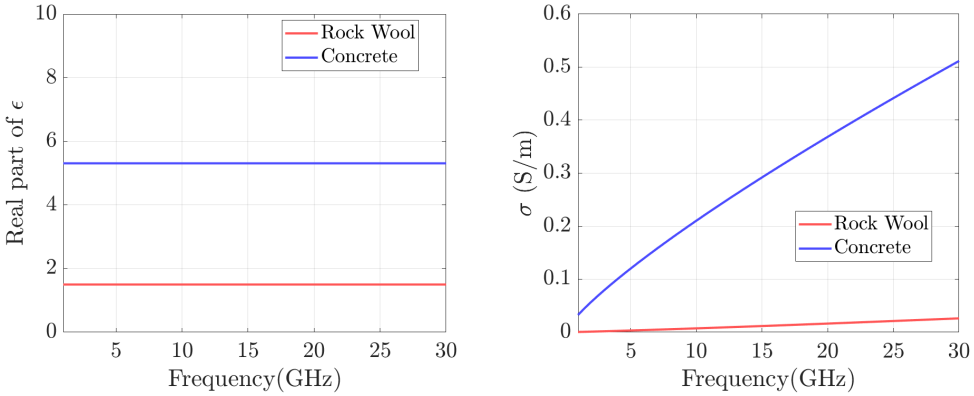

(a) Building materials dielectric constant from 1 to 30 GHz

(b) Building materials conductivity from 1 to 30 GHz

Figure 3.3: Dielectric properties of rock wool (red) and concrete (blue)

The conductivity varies in frequency more than the dielectric constant, which in this case is constant, and it is what defines how much the material will attenuate the radio-waves. Looking at Figure 3.3 is possible to see how fast increase the conductivity when the frequency is higher. The attenuation (L), is defined in chapter 2 equation 2.3:

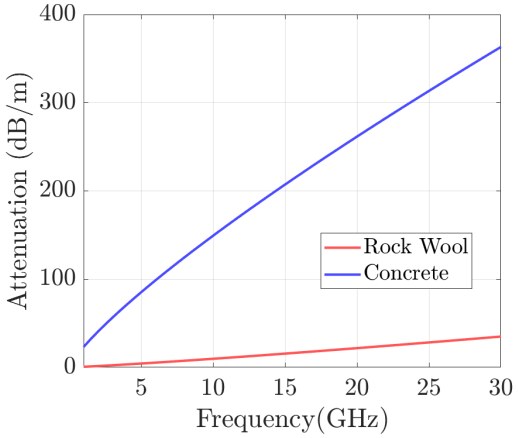

Figure 3.4: Rock wool (red) and Concrete (blue) attenuation

Another parameter interesting to study, to get more insights about how much affect each material to radio waves propagation, is the attenuation, measured in dB/m. In Figure 3.4 we see that concrete attenuation is much higher than the rock wool. This is because rock wool from the electromagnetic point of view is similar to air, which does not attenuate the radio-waves. In the other hand, concrete has a high quantity of water which involves more losses.

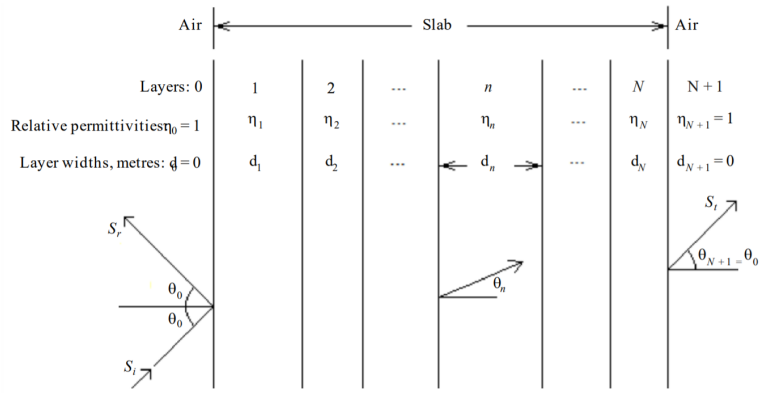

Figure 3.5: Schematic of plane wave reflection and transmission for multi-layer slab [1]

3.2. Building wall analysis and simulation methodology

As explained at the beginning of this chapter, the load-bearing wall model chosen in this thesis is based on three layers. In this section, we first derive an analytical EM model of the structure, based on a general method for a infinite multi-layer dielectric slab described in [1]. Additionally an electromagnetic 3D full-wave simulation is carried out with CST, which is later also used to design the antenna system embedded in the wall.

3.2.1. Load-bearing wall analytical EM model

The model considers a plane wave incident upon a slab consisting of N layers, each layer consists of homogeneous dielectric material and the interfaces are planar, smooth and parallel surfaces. The schematic for the general case is shown in Figure 3.5.

Reflection and transmission are calculated through the following recursive algorithm implemented in MATLAB:

First initialise:

$$A_{N+1} = 1 \quad B_{N+1} = 0 \quad F_{N+1} = 1 \quad G_{N+1} = 0 \tag{3.3a-d}$$

Then for n=N,..,0, being N the number layers:

$$A_n = 0{,}5 \exp jk_n d_n \cos\theta_n [A_{n+1}(1 + Y_{n+1} + B_{n+1}(1 - Y_{n+1})] \tag{3.4a}$$

$$B_n = 0{,}5 \exp jk_n d_n \cos\theta_n [A_{n+1}(1 - Y_{n+1} + B_{n+1}(1 + Y_{n+1})] \tag{3.4b}$$

$$F_n = 0{,}5 \exp jk_n d_n \cos\theta_n [F_{n+1}(1 + W_{n+1} + G_{n+1}(1 - W_{n+1})] \tag{3.4c}$$

$$G_n = 0{,}5 \exp jk_n d_n \cos\theta_n [F_{n+1}(1 - W_{n+1} + G_{n+1}(1 + W_{n+1})] \tag{3.4d}$$

with W_{n+1}, Y_{n+1}, $\cos\theta_n$ and k_n defined as:

$$W_{n+1} = \frac{\cos\theta_{n+1}}{\cos\theta_{n+1}}\sqrt{\frac{\varepsilon_{r\,n+1}'}{\varepsilon_{r\,n}'}} \tag{3.5a}$$

$$Y_{n+1} = \frac{\cos\theta_{n+1}}{\cos\theta_{n+1}}\sqrt{\frac{\varepsilon_{r\,n}'}{\varepsilon_{r\,n+1}'}} \tag{3.5b}$$

$$\cos\theta_n = \frac{\cos\theta_0}{\sqrt{\varepsilon_{r\,n}'}} \tag{3.5c}$$

$$k_n = \frac{2\pi}{\lambda}\sqrt{\varepsilon_{r\,n}'} \tag{3.5d}$$

where λ is the free-space waveglength in metres, $\varepsilon_{r\,n}'$ the dielectric constant of slab n and d_n the width. After evaluting Equations (3.4a) to (3.4d), the E-field reflection and transmission coefficients are related by:

$$R_{TE} = \frac{B_0}{A_0} \quad R_{TM} = \frac{G_0}{F_0} \quad T_{TE} = \frac{1}{A_0} \quad T_{TM} = \frac{1}{F_0} \tag{3.6a-d}$$

where TE means transverse-electric and TM transverse-magnetic incident polarization.

In the particular case of the load-bearing wall model presented in this thesis $N = 3$ and incidence angle θ_0 orthogonal to the slab surface. The dimensions and characteristics are defined in Figure 3.6 and in Table 3.2.

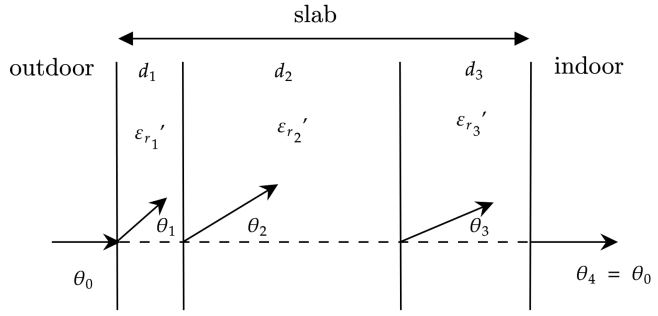

Figure 3.6: Schematic of plane wave reflection and transmission of load-bearing wall model

Table 3.2: Load-bearing wall model dimensions

Material	**Layer number**	d_n **(mm)**
Concrete	1	70
Rock wool	2	200
Concrete	3	150

Taking into account these parameters the transmission and reflection of this wall are computed. The results are shown in Figures 3.7.

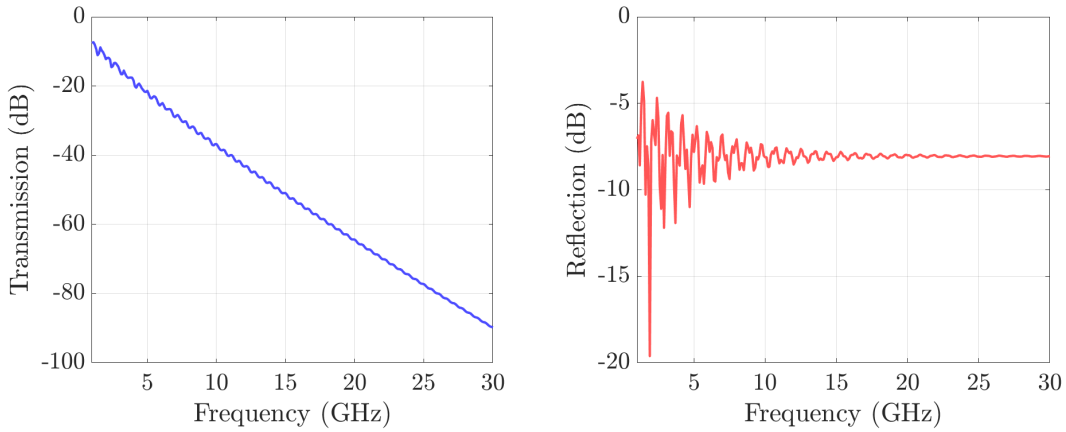

(a) Transmission from 1 to 30 GHz

(b) Reflection from 1 to 30 GHz

Figure 3.7: Plane wave transmission coefficient (blue) and reflection coefficient (red) of load-bearing wall model

It can be seen in Figure 3.7 that in the transmission decreases linearly when frequency increases. At the sub-6 GHz frequency range the attenuation is less than 20 dB. In contrast, at millimeter-wave frequencies the attenuation is higher than 80 dB. On the other hand, the reflection at lower frequencies, as sub-6 GHz region, has high fluctuations, whilst at millimeter-wave is more constant with S_{11} values around -7 dB.

With these conditions, the effect of the antennas, meaning the improvement provided by the antenna system, will be more visible at higher frequencies. First of all, because the wall attenuates more, so any small improvement is more significant. On the other hand, the oscillation of the reflections are smaller and any possible interference between antennas and possibles standing waves will be attenuated by the concrete. However, it is interesting to study the different designs at sub-6 GHz range, because there is less computing capacity needed.

3.2.2. Modelling load-bearing wall with the finite-element simulation method

In this section, a rigorous method for analyzing the load-bearing wall structure th-rough finite-element techniques is presented and detailed.

Floquet theory and boundary conditions configuration

The wall is modelled as an infinite periodic in two dimensions multi-layer structure. The wall is illuminated by a plane wave of wave vector $\mathbf{k} = (k_x, k_y, k_z)$ as shown in Figure 3.8. The software utilized is CST with its frequency-domain solver. To reduce the studied domain to an elementary cell we use Floquet theory. Floquet's theorem means using periodic boundary conditions which involve the periodicity of the fields, which fulfill [9]:

$$f(x + T_x, y, z) = f(x, y, z)e^{-jk_x T_x} \tag{3.7a}$$

$$f(x, y + T_y, z) = f(x, y, z)e^{-jk_y T_y} \tag{3.7b}$$

for a $e^{j\omega t}$ time dependency and T_x, T_y the geometrical structure period, also called unit cell size. As mentioned at the beginning of this chapter, the steel-bar structure dimensions will limit the dimension of the unit cell and from that, $T_x = T_y$. For each proposed solution the unit cell dimension is analyzed and presented in Chapters 5 and 6.

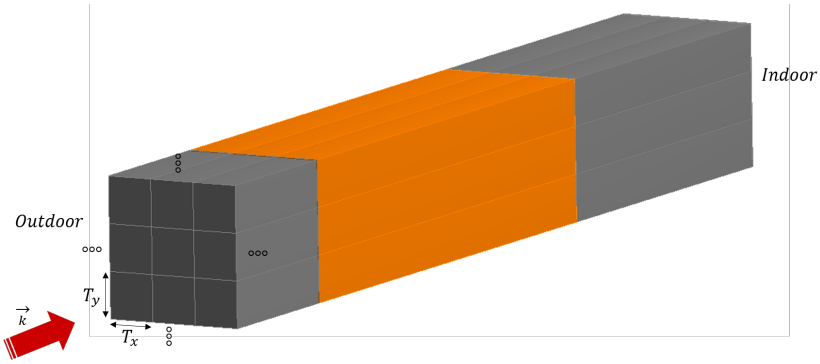

Figure 3.8: Infinite periodicity of the wall model illuminated with an orthogonal plane wave

There are different parameters to configure, the number of modes at each port, the incidence angle of the excitation plane wave and the direction (inward or outward) of the plane wave.

The Floquet modes are the fields at the boundary conditions. In this configuration the number of modes, that the simulation will take into account, is possible to be defined. To avoid loss information, the number of modes is set to 18 at each port. Higher the mode order, less power it will transmit. The total power transmitted from all the modes is calculated from Eq. 3.8.

$$P_t = \sqrt{\sum |S_{21}|^2} \tag{3.8}$$

The structure is excited by a plane wave from the outdoor of the wall. The incidence angle, either ϕ and θ direction, of this plane wave may be changed, by default in this work the plane wave is orthogonal to the wall surface, but there is a parametric study about how the power transmitted changes with the incidence angle of the excitation. The plane wave direction is always outward.

Material definition

In CST there are different way to add a new material,i.e. using dielectric dispersion model as could be Debye model, in this work we add the electrical properties of the materials needed in the selected frequency range from the regression model mentioned in Section 3.1.

Wall simulation and comparison with analytical model

After having defined both analytical and simulation method, Figures 3.9 and 3.10 show transmission and reflection coefficients and the agreement between both methods at two frequency ranges, sub-6 GHz (2 to 7 GHz) and millimeter-wave (24 to 30 GHz).

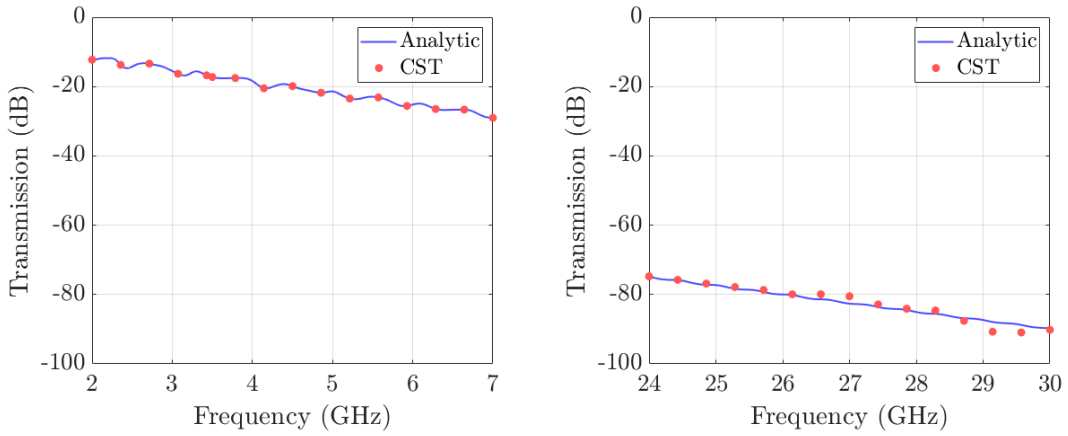

(a) Transmission from 2 up to 7 GHz

(b) Transmission from 24 to 30 GHz

Figure 3.9: Plane wave transmission coefficient of load-bearing wall model analytical and finite-element comparison from 2 to 7 GHz (right) and from 24 to 30 GHz (left)

The transmission, as analytical results shows, is much lower at millimeter-wave, Figure 3.9b band than at sub-6 GHz Figure 3.9a, this is mainly because concrete attenuation is much important at higher frequency as mentioned at the begging of this chapter. In both cases the agreement between analytical and simulation method is good.

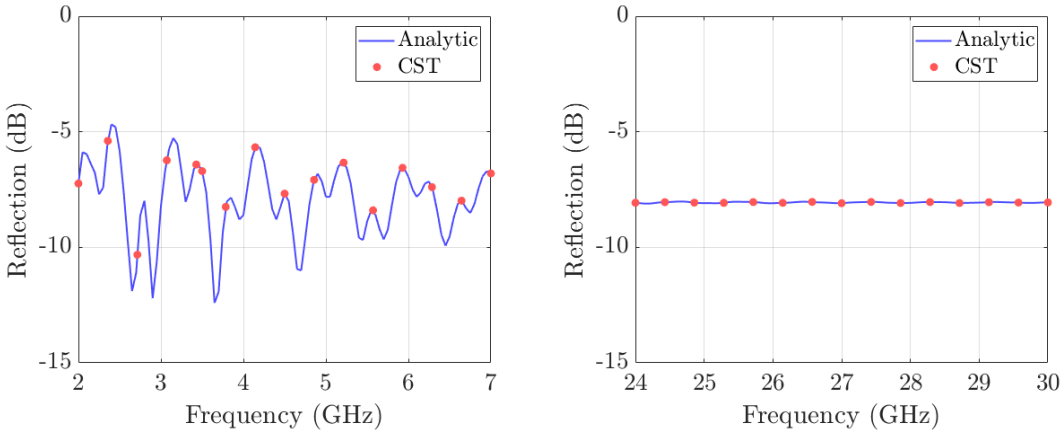

(a) Reflection from 2 up to 7 GHz

(b) Reflection from 24 to 30 GHz

Figure 3.10: Plane wave reflection coefficient of load-bearing wall model analytical and finite-element comparison from 2 up to 7 GHz (rigth) and from 24 to 30 GHz (left)

In the reflection coefficient, there is also consistency between analytical and simulation methods. At sub-6 GHz (Figure 3.10a) the fluctuations are very important if we compare with millimeter-wave (Figure 3.10b) where the reflection is almost constant in that frequency range. This is because the multiple reflections, at higher frequencies, are attenuated by the concrete.

Chapter 4

Solutions for RF transmissive walls

In this chapter the two proposed solutions are explained. On each proposed design there are four key points to study:

1. **Wall antenna density or unit cell width**: the closest the antennas can be is an important parameter to study. It has to take into account the metal net geometry used in the outdoor reinforced concrete wall, which mesh size is typically 150 mm. There is a trade-off between the transmission improvement and the unit cell width, i.e. antenna density, for for obvious reasons.
2. **Transmission improvement**: The goal of the project is improve the transmission so, the amount of improvement of the transmission compared to an unaltered wall is one of the figures of merit.
3. **Bandwidth**: 5G signals have many frequency ranges available both at sub-6 GHz and at millmeter-wave, the antenna should be able to work at both frequency ranges, it can be implemented by having either ultra-wideband or multi-band antenna
4. **Thermal and structural impact of adding the proposed antenna system into the wall**: This project does not focus on that, but we anyway discuss the potential thermal or structural impact of the antenna system.

4.1. Antenna Patch

The first solution proposed utilises two or four microstrip patch antennas. It is well known that the main drawback of the patch is its narrow bandwidth. However, it has the advantage that it is simple to design and also, because of its flat geometry it can be embedded easily into the walls.

There are two possible setups, the first one is one patch in the outer wall connected to another patch in the inner wall through a coaxial cable. The other setup uses four antennas, one in each interface of the different wall layers, and a coaxial cable in each of the concrete sections. The PCB substrate used in both cases is lossy Rogers RO3003.[a]nd

copper is used for the patch and the ground plane.

4.1.1. Two patches and a coaxial cable through the complete wall

In that case, the coaxial cable passes through the whole wall, as depicted in Figure 4.1. The copper in the coaxial cable is a very good thermal conductor, because of that having the coaxial going through the wall creates an undesired heat-bridge from indoor to outdoor. This is one of the effects of the system that must be avoided. Nevertheless, is important to have a reference level of possible improvement and, from this reference try to improve the design. The second improved setup is proposed in 4.1.2 and it intends to avoid any heat bridge.

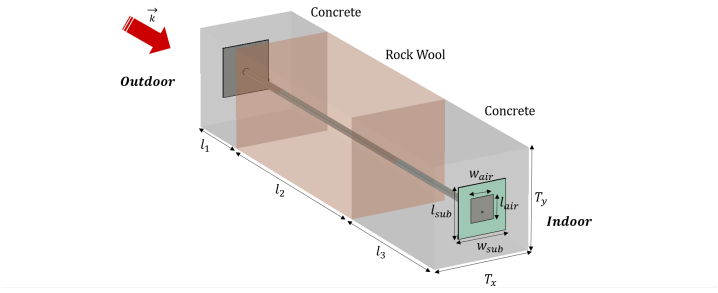

Figure 4.1: Two antenna patches connected through a coaxial schematic

4.1.2. Four patches and coaxial cables through the concrete layers

The improvement of this configuration is based on taking advantage of the rock wool's low attenuation waves and, also low thermal conductivity. Having the coaxial passing through the concrete layers we have still the insulation layer of rock wool without any heat bridge.

In this case, there are four patches: the first patch matched to air facing to outdoor, connected through a coaxial cable to the second patch, this one is matched to rock wool and is radiating inside the rock wool. The third antenna is also matched to rock wool facing the second one. Finally, the third antenna is connected through a coaxial cable to the fourth patch which is embedded in the indoor wall radiating to the interior of the building. The scheme of this setup is depicted in Figure 4.2.

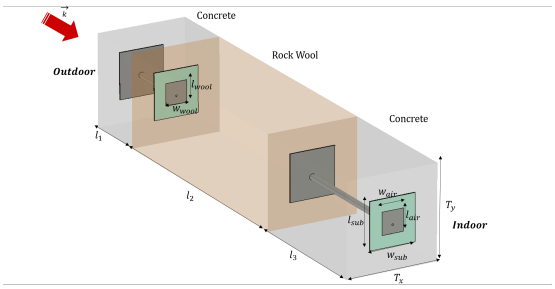

Figure 4.2: Four antenna patches with coaxial through the concrete schematic

With this configuration the thermal insulation should not be affected much, there is no metallic connection from outdoor to the inside the building and, the rock wool acts as the main insulating layer.

4.2. Open Dielectric Waveguide

The second solution proposed is a dielectric waveguide through the complete wall, open on both ends. The main features are its wideband and, by choosing accordingly the dielectrics, the low thermal conduction.

The main difference from a dielectric and the conventional waveguide is that the first one does not contain any metallic structure. Although the conventional may use also dielectric filling to reduce the dimensions, the waveguide itself is metallic.

The dielectric waveguide usually is composed of two parts: the core and the cladding as shown in Figure 4.3. The working principle is based on the total internal reflection (TIR) principle, also used for fibre optics communications. Accordingly, the total internal reflection, the rays inside the core will be guided if $\theta \leqslant \theta_c$, where θ is the incident angle of the ray at the boundary surface and θ_c satisfies [10]:

$$\cos\theta_c = \frac{n_2}{n_1} \tag{4.1}$$

being $n_1 = \sqrt{\varepsilon_1}$ the refraction index in the core and $n_2 = \sqrt{\varepsilon_2}$ in the cladding. To have TIR the indices of refraction must fulfill:

$$\varepsilon_{r1} > \varepsilon_{r2} \tag{4.2}$$

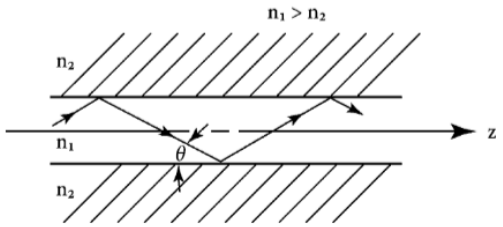

Figure 4.3: TIR principle schematic

Although the materials are chosen satisfying 4.2 there is still field leakage into the cladding. One parameter to study by simulating it is how thick should be the cladding to avoid the leakage pass through the wall and assure that most of the RF power is guided inside the core of the waveguide.

4.2.1. Dielectric material selection

Choosing the material is a key task in order to fulfil the requirements. Besides meeting the TIR principle, the propagation losses are also important, the core material should have low propagation attenuation. As we are trying to avoid any heat bridge is interesting to take into account the thermal conductivity, for example, materials such rock-wool or fibreglass, even though in this project the thermal study is not made.

In this thesis a artificial lossless materials with constant permittivity have been used for the core and the cladding. This was to facilitate the design and study the different parameters needed to be optimized, such as the cladding thickness and the core width.

The core material has dielectric constant of 8 and 0 conductivity whilst the cladding has dielectric constant of 1 and also it is lossless.

4.2.2. Design criteria

For a given working frequency f_c the width of the core has to fulfill:

$$w_{core} = \frac{\lambda_{eff}}{2} = \frac{c}{2f_c\sqrt{\varepsilon_1 - \varepsilon_2}} \tag{4.3}$$

It can be seen in Eq. 4.3 that the dimension depends on the difference between permittivities of core and cladding. The dielectric waveguide frequency cutoff and proper working is really sensitive to any change on this interface. This means that if the cladding thickness is not thick enough the changes outside the cladding, for example the changes at the different layers of the wall will produce changes in the working frequency. The design is illustrated in Figure 4.4.

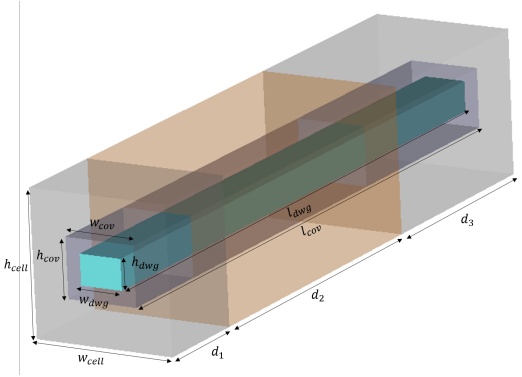

Figure 4.4: Load-bearing model with dielectric waveguide schematic

Some materials proposed to use in a real dielectric waveguide are, fiberglass and rockwool. The first oen for the core, because it has high dielectric constant ($\varepsilon_r' = 6{,}2$), low losses ($tan\delta = 0{,}007$ at $10\,GHz$) [11] and low thermal conductivity ($\kappa = 0{,}06$). Moreover, it is strong enough to withstand the possible forces inside the wall. For the cladding the rock wool is perfect because it is already used as insulator in the construction industry and it has much lower dielectric constant than fiberglass.

Chapter 5

Sub-6 GHz results

This chapter presents the results from the simulations done in the 5G lower frequency range, sub-6 GHz. The main goals of this chapter are to prove the simulation method to compare different designs and, on the other hand, to study the advantages and drawbacks of the different solutions.

5.1. Antenna Patch

The first antenna-system proposed is a patch antenna fed with a coaxial cable, the dimensions of the antenna patch are described in the table 6.1.

Table 5.1: Design dimensions of 3.5 GHz microstrip patch antenna

Parameter	**Abbreviation**	**Dimensions(mm)**
Patch on air width	w_{patch_a}	23.7
Patch on air length	l_{patch_a}	23.7
Patch on rock wool width	w_{patch_r}	23.2
Patch on rock wool length	l_{patch_r}	23.2
Substrate width	w_{sub}	50
Substrate length	l_{sub}	50
Substrate thickness	t_{sub}	1
Metal thickness	t_{met}	0.035

With these dimensions, both setups are simulated and the total power transmitted is plotted to be compared with the power transmitted through the wall without any antenna-system embedded as a reference. The unit cell chosen in this case is 150 mm limited by the steel-structure of the reinforced concrete.

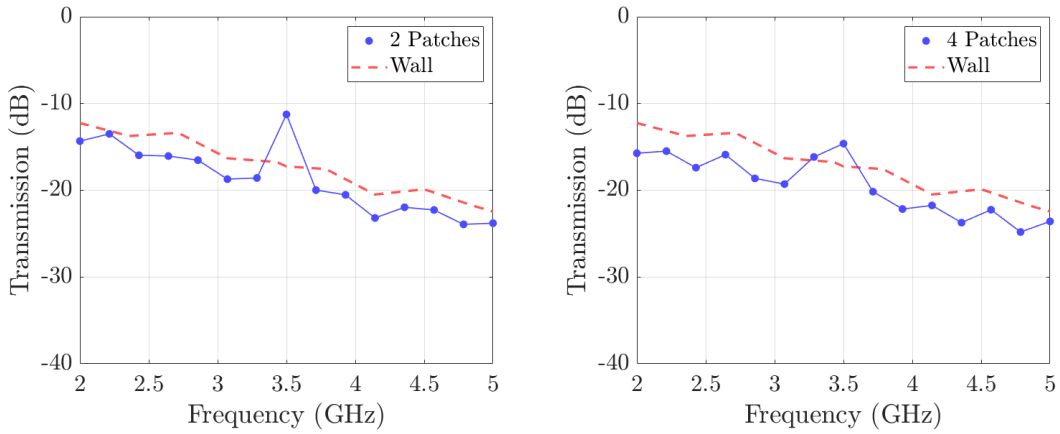

(a) Two patch antennas and coaxial cable through the complete wall

(b) Four patch antennas and coaxial cable just in the concrete layers

Figure 5.1: Transmission coefficient through the load-bearing wall with patch antennas solutions

In Figure 5.1a, there is the setup with the coaxial cable passing through the complete wall, while in the right side, Figure 5.1b, there is the second setup, with the coaxial cable just in the concrete layers. In both figures is clearly shown the narrow bandwidth around 3.5 GHz. Out of this band, the power transmitted is below the reference level (-17.3 dB at 3.5 GHz). The difference is in the level of the power transmitted, in the first case it is -11.3 dB (6 dB of improvement) and in the second case it is -14.6 dB (2.7 dB of improvement) at the working frequency.

As mentioned before, these results are just for the case of 150 mm unit cell size. The density of the antennas embedded in the wall is very important to study. If the density is too high, the improvement in the transmission will be really important but on the other hand, thermal and structural issues may appear. In the opposite situation, if the density is lower, at some point the effect of the antenna will be negligible.

A trade-off between the transmission improvement and the density of the antennas has to be found. To get more insights about how the power transmitted changes with the density of antennas we have made a study of the power transmitted for different unit cell sizes, from 70 mm up to 170 mm, the results are depicted in Figure 5.2.

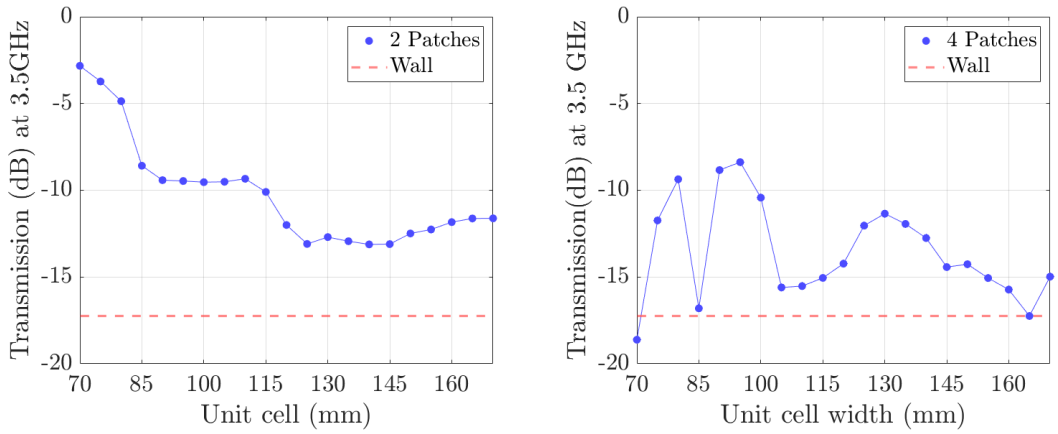

(a) Two patch antennas and coaxial cable through the complete wall

(b) Four patch antennas and coaxial cable just in the concrete layers

Figure 5.2: Transmission coefficient through the load-bearing wall with patches and coaxial through the wall for different unit cell widths

As it can be seen in Figures 5.2a and 5.2b the behaviour of the setups is really different when the unit cell size is changed.

From one side, the setup with the coaxial passing through the whole wall has a trend to decrease the total power transmitted when the unit cell is increased, it is because there is less density of antennas. Even though this decrease is not linear, some smooth fluctuations can be observed, these fluctuations may be due to the waves that, instead of travelling through the coaxial, are passing through the wall. These RF signals passing through the wall are due to the fact that the concrete has not high attenuation at those sub-6 GHz frequencies. In any case, the power transmitted always is above the reference level which means that the improvement is guaranteed at least up to 170 mm unit cell size.

From the other side, the case with the coaxial just in the concrete layers the power transmitted has fast fluctuations and at some points, i.e. $T_x = 70$, 85 and $165\,mm$ the power transmitted is below the reference level. In this situation there are more interference appearing: from side patches, from the wave travelling through the wall and also, inside the rock wool can be an standing wave. This quasi random behaviour is hard to predict and, to get an idea how the power transmitted varies in different cases, we have simulated a random scenario. This random scenario also allows us to experiment the different parameters that the Floquet boundaries has, for example the plane wave incidence angle.

By changing ϕ, θ, the unit cell size and the frequency slightly we will have 125 different scenarios of excitation wave and from that the maximum, mean and minimum value of power transmitted. The different values of the parameters are shown at Table 5.2.

Table 5.2: Parameters that could affect the power transmitted

Parameter	**Sample 1**	**Sample 2**	**Sample 3**	**Sample 4**	**Sample 5**
f (GHz)	3.4	3.45	3.5	3.55	3.6
T_x (mm)	140	145	150	155	160
$\phi(^\circ)$	0	2.5	5	7.5	10
$\theta(^\circ)$	0	2.5	5	7.5	10

The different scenarios options have been simulated and the results have been analysed. From these results, the maximum, minimum and mean value of the transmission coefficient, have been calculated following Eq. 5.1a, 5.1b and 5.1c, and presented in Figure 5.3 in function of the frequency.

$$T_{max} = max(\mathbf{T}) \tag{5.1a}$$

$$T_{mean} = \frac{\sum(T_i)}{N} \tag{5.1b}$$

$$T_{min} = min(\mathbf{T}) \tag{5.1c}$$

where $\mathbf{T}$ is the set of transmission coefficients of each scenario, T_i the transmission coefficient of each scenario and N the number of scenarios.

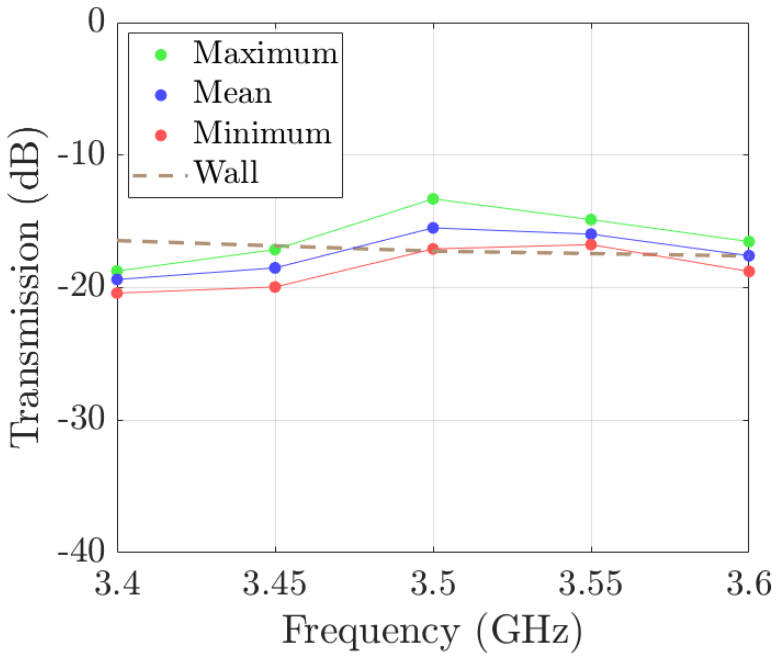

Figure 5.3: Variation of the power transmitted in with the second setup, minimum value (red), mean value (blue), maximum value (green) and reference level (brown)

Checking the behaviour in this small frequency range, from 3.4 to 3.6 GHz, we observe that the bandwidth of this setup is really narrow. At 3.5 GHz and at 3.55 GHz, the

working frequency of the patch, the maximum, mean and minimum transmission is above the reference level. But, out of this band, the mean and minimum value of the transmission coefficient is below the reference level.

From these results we may conclude that in the worst case, at the resonant frequency of the antenna, the transmission will be at least equal to the transmission through the wall without any antenna-system.

5.2. Open dielectric waveguide

To design the dielectric waveguide is more tricky than the patch antenna, because of that the first simulations are done with two test lossless dielectric materials, the core permittivity is 8 and the cladding 2.

Table 5.3: Design dimensions of 3.5 GHz dielectric waveguide

Parameter	**Abbreviation**	**Dimension (mm)**
Dielectric waveguide core width	w_{dwg}	30
Dielectric waveguide core height	h_{dwg}	21
Dielectric waveguide cladding thickness	t_{clad}	10

These dimensions are the ones used to have a first version of the dielectric waveguide and the unit cell in this case is 100 mm trying to reduce the computational cost. After having a reference transmission of this design, we have optimized analyzed the unit cell dimension, the thickness of the cladding and, the matching with air by adding a taper to both waveguide extremes.

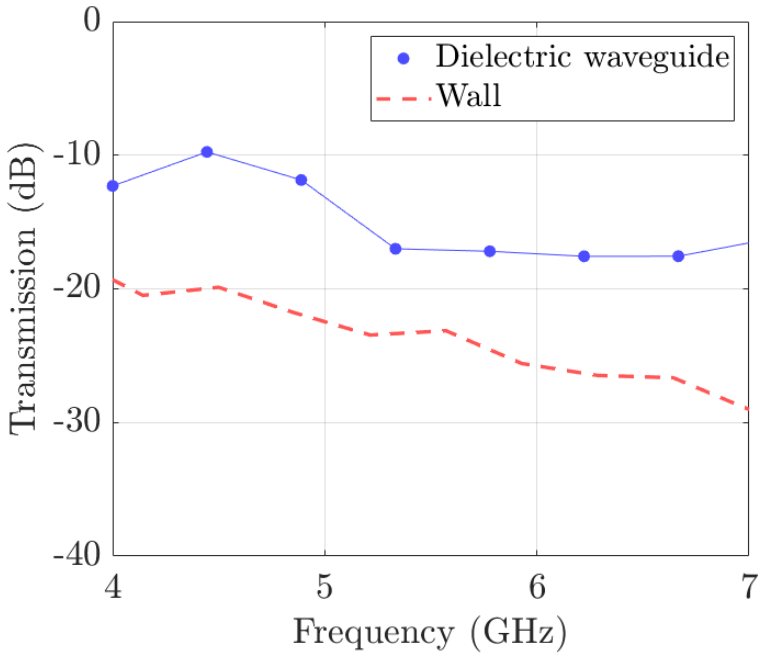

Figure 5.4: Transmission coefficient through the load-bearing wall with open dielectric waveguide

The frequency cutoff of the dielectric waveguide is 3.5 GHz but it starts to work more stable at 4 GHz, because of that we have simulated this frequency range. We observe that the transmission coefficient achieved with this design is more stable and the frequency band where it works is wider. The frequency range is limited due to the computational cost to simulate it.

To be able to compare the dielectric waveguide design with the planar antenna solutions we have simulated also with the same unit cell size as in the planar case, 150 mm (limited by the metal net). The results compared with the unit cell 100 mm is shown in Figure 5.5.

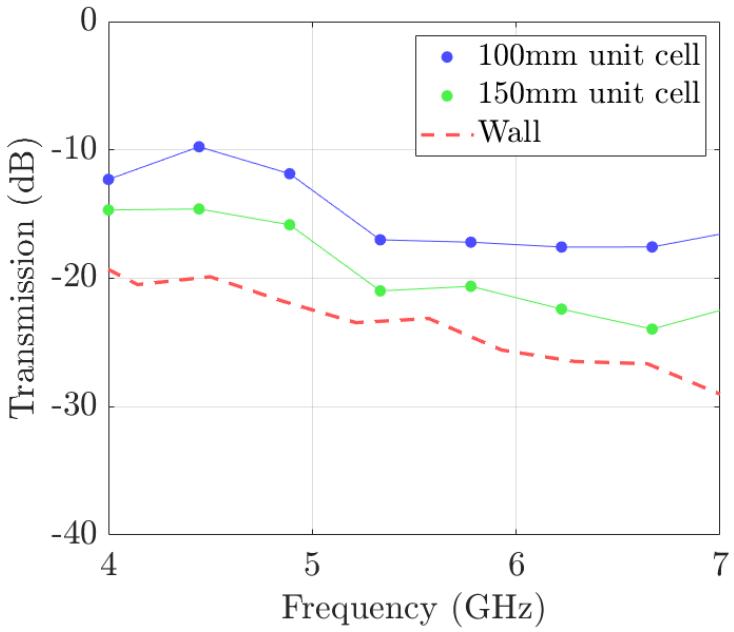

Figure 5.5: Transmission coefficient through the load-bearing wall with open dielectric waveguide for 100 mm (blue) and 150 mm(green) unit cell size

Even by increasing the unit cell, reducing the number of waveguides embedded in the wall, the transmission is improved by around 5dB over the transmission through the wall without any antenna-system. Also, the frequency range where the waveguide works is wider than in the planar case as we could expect.

5.2.1. Cladding thickness parametric study

After having the dielectric waveguide working properly, two different study have been done. The first one, an analysis on the thickness of the cladding, as the leakage that could be in the wall depends on this. Two more cladding thickness have been simulated, 20 mm, and 30 mm. The transmission and reflection coefficients have been simulated and plotted in Figure 5.6.

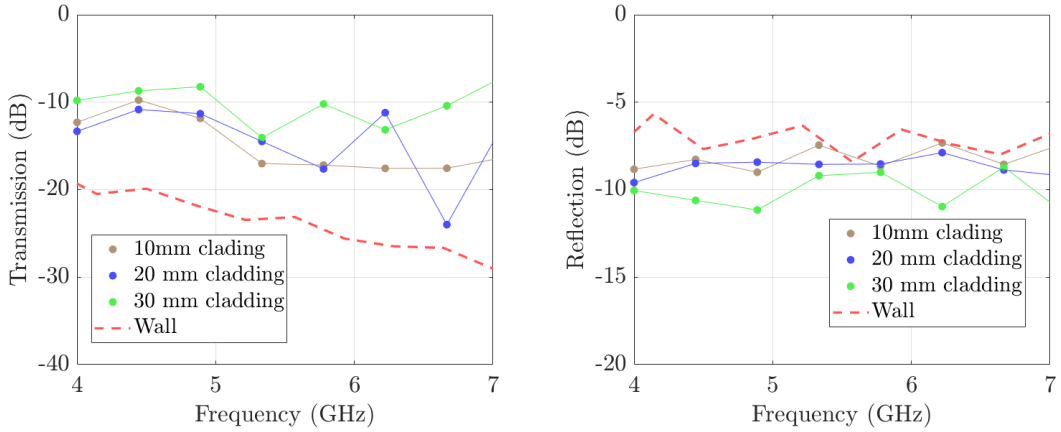

(a) Transmission coefficient

(b) Reflection coefficient

Figure 5.6: Transmission and reflection coefficient through the load-bearing wall with open dielectric waveguide for different cladding thickness

On the left Figure 5.6a the transmission coefficient for the different cases of cladding thickness is shown. There is an improvement in all the cases with respect of the pure wall. Comparing the different cladding thickness we observe that at lower frequency the difference is almost negligible, whilst when the frequency increases, as thicker is the cladding, better is the improvement.

On the right Figure 5.6b the reflection coefficient, for all the cases mentioned above, is presented. In this case, there is an equal improvement in the whole band and we observe that as thicker is the cladding, lower is the reflection. This is due to the permittivity of the cladding is lower than the concrete and core permittivities. The cladding is improving the matching with air.

Another way to improve the matching is adding a matching layer at both extremes of the open waveguide. The proposal to improve the matching is analyzed in Section 5.2.2

5.2.2. Tapper dielectric waveguide

One matching layer in the case of the dielectric waveguides is using a taper at both extremes. this taper has a pyramidic shape of the same core material, that will have a smoother transition between air and the waveguide. This solution is a theoretical solution, as it can not be a practical proposal because of the taper coming out of the wall.

In this work, the taper angle is 50 degrees and 49.4 mm length. The tapered dielectric waveguide scheme is displayed in Figure 5.7.

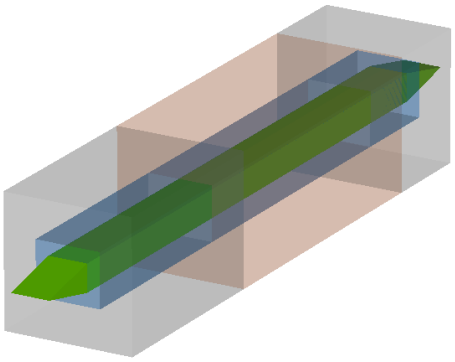

Figure 5.7: Dielectric waveguide taper scheme

The unit cell used in this case is also 100 mm to avoid high computational cost, the claddign thickness is the orginal one, 10 mm. The results are compared with the reference wall and the dielectric waveguide without the taper and, they are exposed in Figure 5.8.

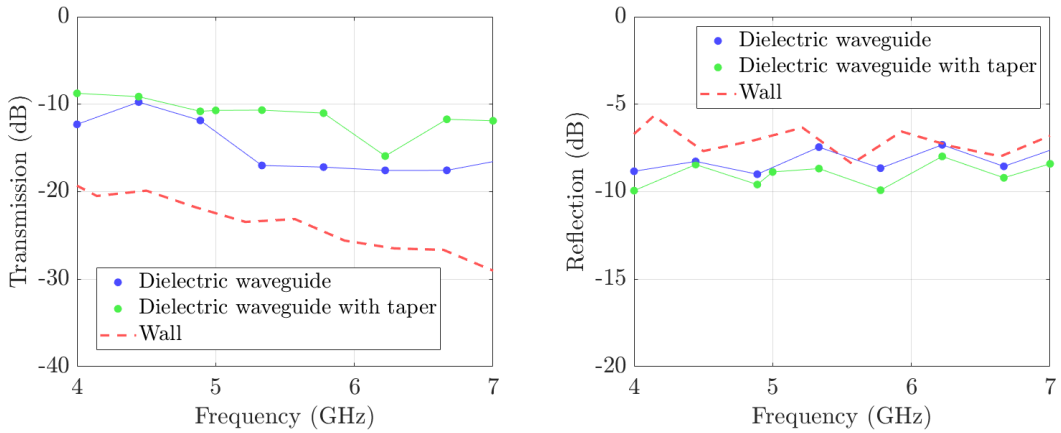

(a) Transmission coefficient

(b) Reflection coefficient

Figure 5.8: Transmission and reflection coefficient through the load-bearing wall with tapered dielectric waveguide

The improvement due to the taper should be reflected directly into the reflection coefficient. Looking at Figure 5.8b is possible to observe there is an improvement, but it is just about 1 or 2 dB. This small improvement in the reflection is translated into the transmission in two different ways. The firs one, at lower frequency there is almost any change. The second one, at higher frequency, the improvement is about 5 dB.

It could be interesting to study wider frequency range to analyze the behaviour more in detail, for example, to see if there are fluctuations in the transmission.

Chapter 6

Millimeter-wave band results

In this chapter a preliminary analysis of both solutions proposed in Chapter 4 at millimetre-wave frequencies is presented. Due to the time cost of each simulation has not been possible to do deeper studies such as how the unit cell size affects at millimetre-wave.

6.1. Antenna patch

In the case of the planar antenna-system solution, both coaxial through the entire wall and coaxial just through the concrete has been analyzed. The dimensions of the antenna patch are described in the table 6.1.

The dimensions of the load-bearing wall are the same, but the unit cell has been resized to have the same ratio as at sub-6 GHz, $T_x = 15\,mm$ and, also to reduce the computational cost, otherwise it was impossible to be simulated.

Table 6.1: Design dimensions of 28 GHz microstrip patch antenna

Parameter	**Abbreviation**	**Dimensions (mm)**
Patch on air width	w_{patch_a}	2.94
Patch on air length	l_{patch_a}	2.94
Patch on rock wool width	w_{patch_r}	2.91
Patch on rock wool length	l_{patch_r}	2.91
Substrate width	w_{sub}	6
Substrate length	l_{sub}	6
Substrate thickness	t_{sub}	0.127
Metal thickness	t_{met}	0.017

These dimensions are for 28 GHz, but after simulate the designs is possible to see that the resonance frequency is slightly shifted to 27.5 GHz. The simulation results are presented in Figure 6.1.

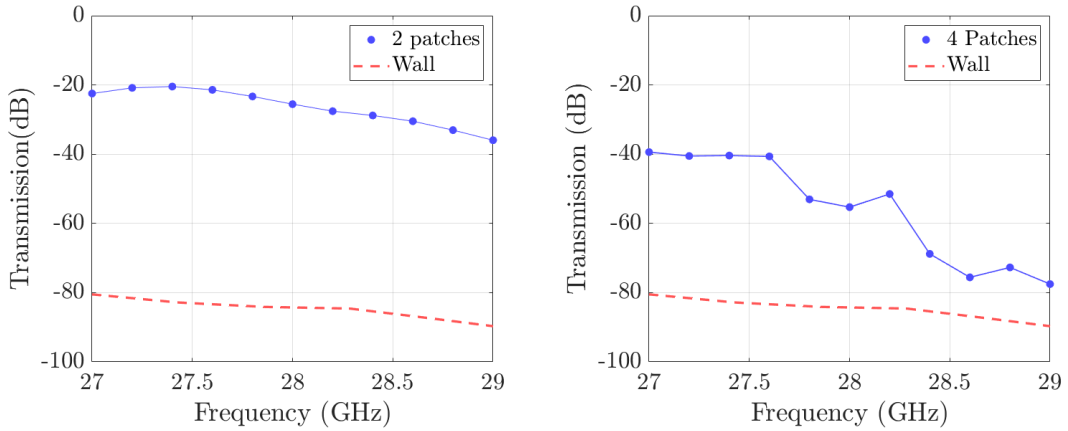

(a) Two patch antennas and coaxial cable through the complete wall

(b) Four patch antennas and coaxial cable just in the concrete layers

Figure 6.1: Total power transmitted through the load-bearing wall with both, coaxial cable through the complete wall (left) and coaxial cable just in concrete layers (right), setups from 27 GHz to 29 GHz

From these figures, the main conclusion is that there is a huge improvement in both setups from 27 GHz to 29 GHz. This was expected due to the high attenuation of concrete at these frequencies, so the small improvements that are presented at sub-6 GHz now are more visible and important.

Even though, the first setup (Figure 6.1a), the coaxial cable passing through the whole wall achieves a transmission coefficient of -20 dB at the centre frequency of the antenna. This transmission is still lower than at sub-6 GHz. It could be interesting to study how the density of the patches affect the transmission in this case.

In the second setup case (Figure 6.1b the behaviour is not as flat as in the first case but the transmission improvement is still visible. First of all the transmission at centre frequency is -30 dB, 10 dB less than in the case with the coaxial through the entire wall. This is due to, from one side to the losses inside the rock wool which at 27.5 GHz is 32 dB/m and the length of the rock wool is 220 mm, which is translated into 7.04 dB. From the other side, There are still 3,difference, what could be the cause?

6.2. Dielectric waveguide

The analysis of the dielectric waveguide at millimetre-wave has not been possible to be done due to capacity limitation. The idea com the dielectric waveguide was to don't need to change its dimensions, utilize the same at sub-6 GHz and millimetre-wave. The problem appears because waveguide dimensions at millimetre-wave are electrically very

large and the computational cost of simulating the wall and the design was too high, and the computers that we have available don't have enough capacity.

Nevertheless, the dielectric waveguide is a theoretical solution as it potentially has structural, thermal and humidity issues.

Chapter 7

Conclusions

The main conclusions that can be extracted from the work developed in previous chapters are summarized in the following lines.

The first conclusion is related to the method that has been developed in this work to have an accurate and efficient way to design different antenna-systems to improve the cellular indoor coverage. Has been proven that the method is useful and efficient at sub-6 GHz band whilst at millimetre-wave frequencies, the computational cost is higher at it should be studied in more detail to reduce it. Nevertheless, at both frequency band, the reference wall was simulated and it was consistent with the analytical model.

The planar solution presented in this work is separated into two different setups, both setups have advantages and drawbacks. The first setup, two antennas embedded one at the outdoor wall and the other one at the indoor wall connected through a coaxial cable, has the advantage that the transmission is more constant due to avoiding the standing waves or reflections inside the rock wool. Also, the transmission improvement is higher than in the second proposed setup. From the other side, the main drawback is the potential structural and thermal issues.

In the case of the second setup, the structural and thermal possible issues are lower as there is no heat bridge from the outdoor to the indoor. But the drawback is that there are multiple reflections, interference and random"behaviour inside the rock wool that is difficult to predict. Despite this, the multi-parametric simulation has shown that the mean value of the transmission is over the reference level of the pure wall.

As the main drawback in both setup of the planar solution, there is the narrow band where the antennas are working.

The second solution proposed was the dielectric waveguide as a non-metallic solution and with this avoiding the heat bridge and trying to don't affect the thermal insulation. The main advantage of the waveguide is the ultra-wideband useful to work at both frequency bands, sub-6 GHz and millimetre-wave. The drawback has been from one side, the computational cost at millimetre-waves and, from the other side, the potential structural problems.

As a global conclusion, there is a need to study an ultra-wideband planar antenna-

system solution and study the impact of both setup explained, the coaxial through the wall or just in the concrete. More future work are detailed in Section 7.1.

7.1. Future Work

This work is just the starting point of a more ambitious project regarding improving the cellular coverage inside buildings for the 5G signals. Besides, some of the proposals have to be optimized before extending the work to other topics. The simulation method at millimetre-wave frequencies should be optimized to reduce the computational cost.

In a mid-term period, there are several proposals to extend this thesis and cover advanced topics. The consideration of structural as well as thermal issues by carrying out multi-physics simulations. It also leads to a study of how the solutions presented in this thesis affects the structural and thermal insulation point of view as well as confirm the hypothesis that the dielectric waveguide is not a practical solution.

The design and analysis of an ultra-wideband planar antenna is also a must to work on it if both frequency ranges must be covered.

In a long-term period different types of walls could be studied and simulated to analyse the impact of them over the RF signals. Finally, the measurement of a real wall to be compared with the methods and assure that it is consistent and it could be used.

This thesis tried to cover some aspects and introduce others for future research lines.

7.2. Research Outcome

This work will be presented in a conference during summer 2020.

Bibliography

[1] I. Rec, "P. 2040-1,âĂIJeffects of building materials and structures on radiowave propagation above about 100 mhz,âĂİ," *Int. Telecommun. Union, Geneva, Switzerland*, 2015.

[2] Y. J. Kim, L. Jofre, F. D. Flaviis, and M. Q. Feng, "Microwave reflection tomographic array for damage detection of civil structures," *IEEE Transactions on Antennas and Propagation*, vol. 51, pp. 3022–3032, Nov 2003.

[3] L. Jofre, A. Broquetas, J. Romeu, S. Blanch, A. P. Toda, X. Fabregas, and A. Cardama, "Uwb tomographic radar imaging of penetrable and impenetrable objects," *Proceedings of the IEEE*, vol. 97, pp. 451–464, Feb 2009.

[4] L. Yujiri, M. Shoucri, and P. Moffa, "Passive millimeter wave imaging," *IEEE Microwave Magazine*, vol. 4, pp. 39–50, Sept 2003.

[5] D. M. Sheen, D. L. McMakin, and T. E. Hall, "Three-dimensional millimeter-wave imaging for concealed weapon detection," *IEEE Transactions on Microwave Theory and Techniques*, vol. 49, pp. 1581–1592, Sep 2001.

[6] "ISO TC 163/SC 2 Building materials and products-Hygrothermal properties-Tabulated design values and procedures for determining declared and design thermal values. ISO/FDIS 10456:2007(E)," 2007.

[7] "Thermal conductivity, specific heat capacity and density."

[8] "Raudoitus."

[9] E. Richalot, M. Bonilla, M.-F. Wong, V. Fouad-Hanna, H. Baudrand, and J. Wiart, "Electromagnetic propagation into reinforced-concrete walls," *IEEE Transactions on Microwave Theory and Techniques*, vol. 48, no. 3, pp. 357–366, 2000.

[10] C. Yeh and F. I. Shimabukuro, *The essence of dielectric waveguides*. Springer, 2008.

[11] V. Sokolov, S. Shalgunov, I. Gurtovnik, L. Mikheeva, and I. Simonov-Emel'yanov, "Dielectric characteristics of glass fibre reinforced plastics and their components," *International Polymer Science and Technology*, vol. 32, no. 7, pp. 62–67, 2005.